Cellular Energy Sensor Sirt1 Augments Mapk Signaling to Promote Hypoxia/Reoxygenation-Induced Catch-up Growth in Zebrafish Embryo

Authors: Hayasaka, Oki, Shibukawa, Mukaze, and Kamei, Hiroyasu

Source: Zoological Science, 41(1) : 21-31

Published By: Zoological Society of Japan

URL: https://doi.org/10.2108/zs230059

ZOOLOGICAL SCIENCE **41**: 21–31 (2024)

Cellular Energy Sensor Sirt1 Augments Mapk Signaling to Promote Hypoxia/Reoxygenation-Induced Catch-up Growth in Zebrafish Embryo

Oki Hayasaka[1†], Mukaze Shibukawa[2,3†], and Hiroyasu Kamei[1*]

[1]*Faculty of Biological Science and Technology, Institute of Science and Engineering, Kanazawa University, Kanazawa, Ishikawa 920-1192, Japan*
[2]*Graduate School of Natural Science and Technology, Kanazawa University, Kanazawa, Ishikawa 920-1192, Japan*
[3]*Ikedamohando Co., Ltd., Nakaniikawa-gun, Toyama 930-0365, Japan*

Animal growth is blunted in adverse environments where catabolic metabolism dominates; however, when the adversity disappears, stunted animals rapidly catch up to age-equivalent body size. This phenomenon is called catch-up growth, which we observe in various animals. Since growth retardation and catch-up growth are sequential processes, catabolism or stress response molecules may remain active, especially immediately after growth resumes. Sirtuins (Sirt1–7) deacetylate target proteins in a nicotinamide adenine dinucleotide-dependent manner, and these enzymes govern diverse alleys of cellular functions. Here, we investigated the roles of Sirt1 and its close paralog Sirt2 in the hypoxia/reoxygenation-induced catch-up growth model using zebrafish embryos. Temporal blockade of Sirt1/2 significantly reduced the growth rate of the embryos in reoxygenation, but it was not evident in constant normoxia. Subsequent gene knockdown and chemical inhibition experiments demonstrated that Sirt1, but not Sirt2, was required for the catch-up growth. Inhibition of Sirt1 significantly reduced the activity of mitogen-activated kinase (Mapk) of embryos in the reoxygenation condition. In addition, co-inhibition of Sirt1- and Igf-signaling did not further reduce the body growth or Mapk activation compared to those of the Igf-signaling-alone-inhibited embryos. Furthermore, in the reoxygenation condition, Sirt1- or Igf-signaling inhibition similarly blunted Mapk activity, especially in anterior tissues and trunk muscle, where the *sirt1* expression was evident in the catching-up embryos. These results suggest that the catch-up growth requires Sirt1 action to activate the somatotropic Mapk pathway, likely by modifying the Igf-signaling.

Key words: sirtuin, mitogen-activated protein kinase (Mapk), insulin-like growth factor (Igf/IGF), zebrafish, embryonic growth, hypoxia, re-oxygenation, catch-up growth

INTRODUCTION

Internal factors control animal growth, but the surrounding environment also influences it. Among such, growth hormone (GH), insulin-like growth factor (IGF/Igf), and thyroid hormones are all major endocrine factors controlling growth and metabolism together with genes involved in skeletal development (Cabello and Wrutniak, 1989; Saenger et al., 2007; Berendsen and Olsen, 2015; Kraemer et al., 2020). On the other hand, external factors, such as nutritional conditions, oxygen concentration, environmental temperature, or toxic substances, also change body growth (Wit and Boersma, 2002; Kamei et al., 2011; Gat-Yablonski and Phillip, 2015). If these conditions are unfavorable, the growth is stunted; however, once the adverse conditions are gone, growth proceeds faster than expected, and the body size often catches up to the age-appropriate level in a relatively short period (Osborne and Mendel, 1915; Wit and Boersma, 2002; Kamei et al., 2011). This phenomenon is called "*catch-up growth*", which occurs widely in vertebrates. In humans, the infant who experiences intrauterine growth retardation catches up to standard height/weight within approximately several months after birth (Saenger et al., 2007). Also, GH administration induces catch-up growth in GH-deficiency patients (Berendsen and Olsen, 2015). In fish, catch-up growth has been observed not only during the juvenile stages but also during the pre-hatching embryonic stage (Kamei et al., 2011). Although catch-up growth commonly appears across taxa, the unified molecular mechanism to explain how this occurs is still obscure.

The zebrafish embryo is an excellent model for studying molecular and cellular mechanisms of normal growth,

* Corresponding author. E-mail: hkamei@se.kanazawa-u.ac.jp
† These authors contributed equally to this work.
doi:10.2108/zs230059

growth retardation, and catch-up growth in developing embryos (Kimmel et al., 1995; Kajimura et al., 2005; Kamei et al., 2011; Kamei and Duan, 2018; Kamei et al., 2018). Previous studies have shown that significant growth retardation and subsequent catch-up growth appeared in zebrafish embryos simply by temporarily reducing the oxygen level of the environmental rearing water and then returning the embryos to the water with normal oxygen concentration (Kamei et al., 2011; Kamei and Duan, 2018). These studies revealed that modification of the Igf-signaling is vital to catch-up growth. Namely, even though there is no change in the activation of the functional cell surface receptor for Igf-ligands (type-1 Igf-receptor or Igf1r), the Mapk-signal transduced by the Igf1r increased. Likewise, the growth-promoting function of the Mapk was augmented in catch-up growth. Notably, the Igf-Pi3k pathway was not distinct between normal and catch-up growth. Recent findings revealed that the insulin receptor substrate 2b (Irs2b), a signaling hub molecule acting immediately downstream of Igf1r, was responsible for this biased Igf-Mapk pathway (Zasu et al., 2022). However, it remained unclear how the Irs2b function is uniquely altered in the catch-up growth. In the growth retardation caused by prolonged hypoxia, lower energy or ATP level leads to starvation-like catabolic conditions at the cellular, tissue, and individual levels (Kajimura et al., 2005; Kamei et al., 2008; Guarente, 2009; Clemmons, 2018; Kamei, 2020). Thus, a cellular energy sensor may play a role, if partial, to uniquely modify the Igf-Mapk pathway in the zebrafish model.

Sirtuin (SIRT/Sirt) is the ortholog of Silent information regulator 2 (Sir2) firstly discovered in yeast (Kaeberlein et al., 1999). SIRT is a nicotinamide adenine dinucleotide (NAD)-dependent protein deacetylase widely conserved in eukaryotes (Imai et al., 2000). SIRT becomes active under catabolic conditions such as starvation, and changes its cellular energy metabolism (Sauve, 2010). Therefore, SIRT is also called an “energy sensor” and is considered one of the master molecules regulating cellular energy homeostasis (Imai et al., 2000; Chang and Guarente, 2014; Madsen et al., 2016). In mammals, there are paralogs from SIRT1 to SIRT7, of which SIRT1 has been the most studied molecule (Houtkooper et al., 2012). At the organismal level, recent studies in Planaria have shown that SIRT1 is also required for growth by modifying feeding behavior and organogenesis (Ziman et al., 2020). Furthermore, cartilage-specific *Sirt1* gene knockout also showed that Sirt1 plays a key role in catch-up growth in a rodent model (Shtaif et al., 2020). However, because systemic knockout mice of this gene cannot survive longer after birth (McBurney et al., 2003), a comprehensive understanding of how SIRT1 governs global body growth in early embryos remains elusive.

Regarding the molecular functions, SIRT1 modifies a wide range of target proteins in the nucleus and cytoplasm: histones, p53, fork head box-containing protein O sub-family 1 (FOXO1, a core transcription factor in the regulation of glucose metabolism, insulin activity, and mitochondrial ATP production), peroxisome proliferator-activated receptor gamma coactivator 1-alpha (PGC1α, a transcription cofactor required for mitochondrial biosynthesis), and insulin receptor substrate (IRS, a molecular hub of insulin and IGF-signaling) are major deacetylation targets of Sirt1 (Michishita et al., 2005; Houtkooper et al., 2012; Lee and Goldberg, 2013; Chang and Guarente, 2014; Rifai et al., 2018). Indeed, SIRT1 promotes the deacetylation of IRS2, resulting in increased signaling in the IGF-Mapk pathway (Li et al., 2008). During growth retardation induced by hypoxia, the cell is likely in catabolic status. It is possible that the function of Sirt1 and related proteins remains active at the beginning of catch-up growth and contributes to its characteristic growth spurt. Sirt1 and other paralogs Sirt2 and Sirt3 belong to class-I Sirtuins. Sirt1 and Sirt2 are located in the cytosol and nucleus, but Sirt3 is located in the mitochondria (Kincaid and Bossy-Wetzel, 2013). Augmentation of the Igf1r-Mapk pathway promotes hypoxia/reoxygenation-induced catch-up growth. The Igf1r-activation is initiated in the cytosol (or near its plasma membrane), and the active-Mapk phosphorylates cytosolic/nuclear substrates. Thus, we focused on Sirt1 and Sirt2, which show nuclear and cytoplasmic localization.

Here, in this study, we aimed to clarify the roles of Sirt1 and one of its closest paralogs, Sirt2, in catch-up growth using zebrafish embryos. First, we conducted pharmacological and genetic blockade of Sirt1/2. Next, the molecular mechanism of Sirt1 was examined to test if it regulates the Igf-Mapk pathway in the reoxygenation-induced catch-up growth. We also examined the expression levels of *sirt1* and its functional domains. The current study will shed light on understanding cellular energy homeostasis and embryonic growth from an endocrinological perspective.

MATERIALS AND METHODS

Animals

Zebrafish (AB strain) were supplied by Zebrafish International Resource Center (ZIRC, Oregon, USA). Adult zebrafish were reared in a rectangular tank (1.3 L) under a 14-hour light/10-hour dark-light cycle, and the water temperature was maintained at 28.5 $\pm$ 1.0°C. Formulated feed or *Artemia nauplii* was fed to fish twice a day. Fertilized eggs were obtained from natural crosses. All experiments were conducted following the guidelines for the care and use of animals at Kanazawa University and were approved by the Committee on Animal Experimentation of Kanazawa University (protocol # 6-2398).

Hypoxia and reoxygenation

Hypoxic water was prepared as described previously (Kamei and Duan, 2018). Briefly, the embryo-rearing solution (E3) was bubbled with pure nitrogen gas to create hypoxic water (Kamei and Duan, 2018). Oxygen concentrations were measured using a dissolved oxygen meter (YSI model ProODO, YSI Nanotech Japan, Kawasaki, Japan). In the control group, all embryos were reared in a stable normoxic environment (**Norm**, 8.0 $\pm$ 1 mgO_2/L). The experimental group was maintained in Norm water until 24 hpf, then exposed to hypoxic water (**Hypo**, 0.8 $\pm$ 0.1 mgO_2/L) for 12 h and returned to normoxic water (reoxygenation condition, **Reoxy**).

Growth measurement

Head-trunk angle (HTA) indicates embryonic body growth (Kimmel et al., 1995). HTA was measured by previously described methods (Kimmel et al., 1995; Kamei et al., 2011). The growth rate was calculated using the following formula: $dh/dt = (h_n - h_0)/(t_n - t_0)$; h_0: HTA at an initial time point (t_0), h_n: HTA at the end time point (t_n). The relative growth rate was calculated as the percentage of the growth rate of the control group. Comparison of the growth rate of normally growing embryos and catching up embryos at the same chronological age was used to evaluate the stage-mismatched growth rate. Each developmental stage should have unique devel-

opmental gene expression, which would make understanding of the growth-promoting factors more complex. Therefore, to avoid this problem, we decided to compare growth rates of "stage-matched" embryos instead of age-matched embryos.

Microinjection of antisense morpholino oligo (MO)

To knock down *sirt1* and *sirt2*, antisense MO against zebrafish *sirt1* mRNA (*sirt1* MO: 5′- CGAACCAAACTCACCAATCTGTGGC-3′), and against zebrafish *sirt2* mRNA (*sirt2* MO: 5′- ACCTCTAAAGGACACAAAAAAGGCT-3′) were purchased from Gene Tools, LLC (Philomath, OR, USA). MO or common control MO (5′-CCTCTCTTACCTCAGTTACAATTTATA-3′) was injected into one- or two-cell-stage embryos (1-4 ng/embryo: 4 ng for *sirt1* MO and control MO, 1 ng for *sirt2* MO and control MO) using Nanoject III (Drummond Scientific Company, Broomall, U.S.).

Chemicals and reagents

Sirtinol (SIGMA-Aldrich, Tokyo, Japan) is a selective inhibitor of both Sirt1 and Sirt2. EX-527 (Abcam, Cambridge, UK) is a Sirt1-specific inhibitor. AK-1 (Abcam) is a Sirt2-specific inhibitor. BMS754807 (Selleck, Tokyo, Japan) is an Igf1r inhibitor. All chemicals were aliquoted and stored at –80°C until each experiment. Each chemical was dissolved in dimethyl sulfoxide (DMSO) and exposed to the embryo at 26 hpf to 36 hpf (Norm) or 36 hpf to 48 hpf (Reoxy). 0.2% DMSO was used as vehicle treatment.

Whole-mount in situ hybridization

Based on Potente et al. (2007), a partial *sirt1* sequence cDNA was cloned. To make an RNA probe, we designed sets of primers (*sirt1*-probe-F:5′-CGCGGGAATTCGATTGACTGCTCATCCCGTGCCAG-3′ and *sirt1*-probe-R:5′-AATTCACTAGTGATTGGCTTCACAGTCCACCTTAT-3′). The probe sequence was inserted downstream of the T7 promotor of the pGEM vector, and in vitro transcription was performed using SP6 or T7 RNA polymerase (Promega K.K, Wisconsin, U.S.) with a 10 × DIG RNA Labeling Mix (Roche Diagnostics, Basel, Switzerland). The synthesized RNA probes were purified using lithium chloride. For hybridization, embryos were fixed with 4% paraformaldehyde (PFA) for 30 min after replacement with 100% MeOH at –20°C. Subsequently, the sample was incubated in a series of decreasing MeOH concentrations in MeOH/PBST (0.8% NaCl, 0.02% KCl, 0.02M PO_4, 0.1% Tween 20) and treated with Proteinase K (Roche Diagnostics). Hybridization was performed overnight at 65°C, and the signal was detected using an anti-DIG antibody (1:5000, Roche Diagnostics). The image was obtained using a stereo microscope (SZX16, Olympus Corporation, Tokyo, Japan).

Real-time-quantitative PCR (RT-qPCR)

Total RNA was extracted from a minimum of 10 embryos after homogenization in a 1.5 mL tube with 500 μL Trizol Reagent (Thermo Fisher Scientific Inc., Massachusetts, U.S.) following the manufacturer's instructions. SuperScript II RNase H - Reverse Transcriptase (Thermo Fisher Scientific Inc.) was used for cDNA synthesis, and TaKaRa Taq-DNA polymerase (Takara Holdings Inc., Shiga, Japan) was used for reverse-transcription PCR (RT-PCR). TB Green Premix Ex Taq II (Takara Holdings Inc.) was used for real time-quantitative PCR (RT-qPCR). To confirm gene expression, we designed two primer sets for RT-qPCR (*sirt1*: 5′-ACTGATGAAGGTGTTCATCCCA-3′ and 5′-GAGATGTTGATGATGATCTGCCA-3′), (*sirt2*: 5′-GCTGGCTTATAGTTTTAAAGAGGGTA-3′ and 5′-AGTATGTAGCGAGCAACTGAGTC-3′). *β-actin* was used as an internal control to normalize gene expression for quantitative RT-PCR (*β-actin*: 5′-CACGAGACCACCTTCAACT-3′ and 5′-ATCCAGACGGAGTATTTGC-3′). The RT-qPCR data was calculated by the standard curve method.

Western blotting

The western blotting assay was carried out as described previously (Kamei et al., 2018). In brief, embryo extracts were prepared from a minimum of 10 embryos after homogenization in the lysis buffer. The embryo extracts were resolved by sodium dodecyl sulfate-polyacrylamide gel electrophoresis (SDS-PAGE) and were then transferred to a polyvinylidene difluoride (PVDF) membrane. The PVDF membrane was blocked with PVDF Blocking Reagent of the Can Get Signal (TOYOBO Co., LTD. Oosaka, Japan) for 2 hours at 37°C and the following primary antibodies were used: anti-total-Erk1/2 (#137F5, 1:1000, Cell Signaling Technology-Japan, Tokyo, Japan) or anti-phospho-Erk1/2 (#9101, 1:1000, Cell Signaling Technology-Japan) overnight at 4°C. A secondary antibody was used: anti-Rabbit-IgG (#55678, 1:10,000, CosmoBio, Tokyo, Japan), for 2 hours at room temperature. The signal was detected using a Western Lightning Plus-ECL kit (Perkin Elmer-Japan, Kanagawa, Japan) with X-ray film (Super RX; FUJIFILM, Tokyo, Japan). Every step was done according to the manufacturer's protocol. The resulting images were analyzed using ImageJ software, and the Mapk activity was calculated as phospho-Erk1/2 signal divided by total-Erk1/2 signal.

Whole-mount immunostaining

Embryos were fixed in 4% PFA overnight at 4°C. After fixation, the samples were kept in 100% MeOH at –20°C. The samples were soaked in a series of MeOH and acetone at –20°C to permeabilize the tissue. Embryos were incubated with PBDT (PBS, 1% BSA, 1% DMSO, 0.1% Tween 20) containing 2% newborn bovine serum for 30 min at room temperature to block non-specific binding sites. After blocking, the embryos were incubated with 1st antibody (anti-phospho-Erk1/2, #9101, 1:1000, Cell Signaling Technology-Japan, Tokyo) overnight at 4°C. Embryos were then incubated overnight with the 2nd antibody (Goat Anti-Rabbit-IgG H&L DyLight 594, ab96901, 1:250, Abcam) at 4°C. Signals and images were observed using a confocal laser microscope (FV10i, Olympus).

Statistics

The results are shown as mean ± SD. *P*-value less than 0.05 was considered statistically significant. The student's t-test (Figs. 2A, 3A, 4B) or Mann-Whitney U-test (Fig. 5B, and see Supplementary Figure S2B) was used to compare two groups. Multiple comparisons were made using one-way ANOVA, followed by Tukey's multiple comparisons test (Figs. 1B, 2B, 3B, and 6). All data sets were calculated using GraphPad Prism 9.

RESULTS

Pharmacological blockade of Sirt1/2

We examined whether exposure to Sirtinol affects rapid growth acceleration under the Reoxy condition (36 hpf to 48 hpf) and under the Norm condition (26 hpf to 36 hpf) at the same embryonic growth stage. All concentrations of Sirtinol had no effects on embryonic growth under the Norm condition (Fig. 1B). Under the Reoxy condition, the Sirtinol treatment significantly reduced the growth of embryos in a dose-dependent manner (Fig. 1B). Among the concentrations tested, we observed significant growth reduction in the 50 μM Sirtinol-treated group compared to the control (54.4 ± 7.8%, Fig. 1B).

Gene-specific knockdown of *sirt1* and *sirt2*

To investigate whether the catch-up growth requires *sirt1* or *sirt2*, we used splicing block morpholino antisense oligos (MOs). To verify the effect of the MOs, we carried out an RT-PCR analysis. *sirt1*-MO induced splicing block at the exon 2 and intron 2 boundary (see Supplementary Figure

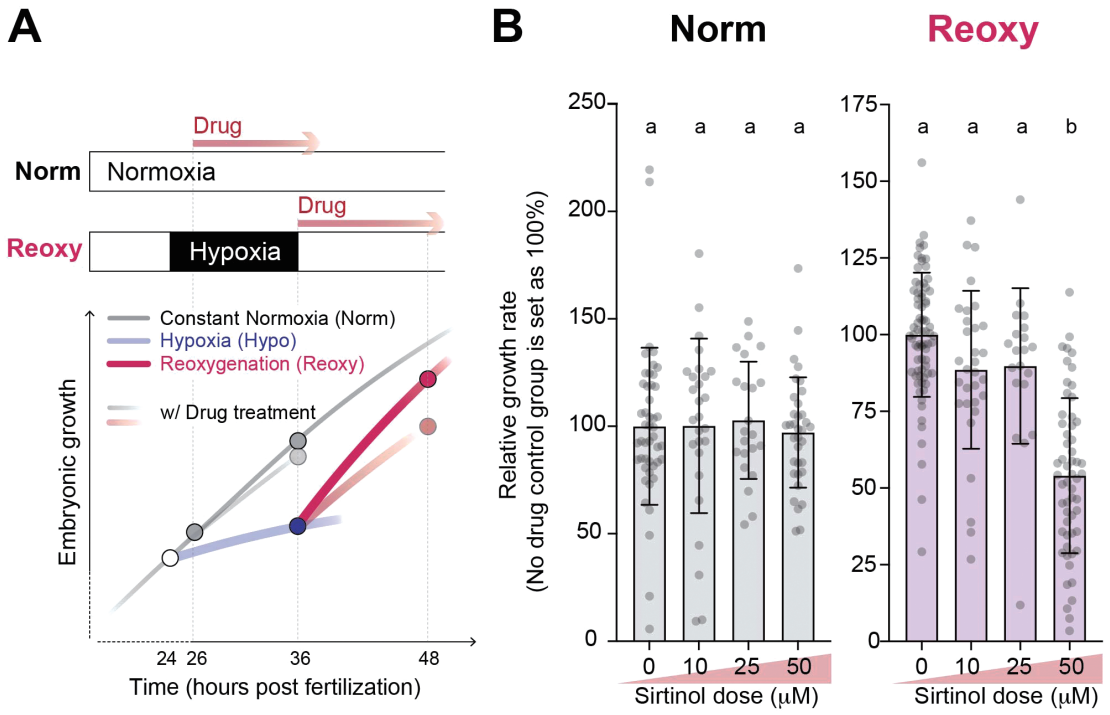

Fig. 1. Temporal blockade of Sirt1/2 in embryos growing under constant normal oxygen condition (Norm) and re-oxygenation condition (Reoxy). **(A)** A diagram showing outline of drug exposure experiments. Sirtinol simultaneously inhibits both Sirt1 and Sirt2 in Norm and Reoxy conditions. Embryos in comparable growth stages were treated with Sirtinol, and the growth rate was analyzed. **(B)** Changes in growth rate of the Sirtinol-treated embryos in Norm and Reoxy conditions. The control group (DMSO) was set as 100. Values shown are mean ± SD. Data were obtained from two–four independent assays. n = 47 (Norm DMSO); n = 27 (Norm Sirtinol 10 μM); n = 22 (Norm Sirtinol 25 μM); n = 35 (Norm Sirtinol 50 μM); n = 74 (Reoxy DMSO); n = 31 (Reoxy Sirtinol 10 μM); n = 20 (Reoxy Sirtinol 25 μM); n = 57 (Reoxy Sirtinol 50 μM). Different letters mean statistical significance at $P < 0.0001$.

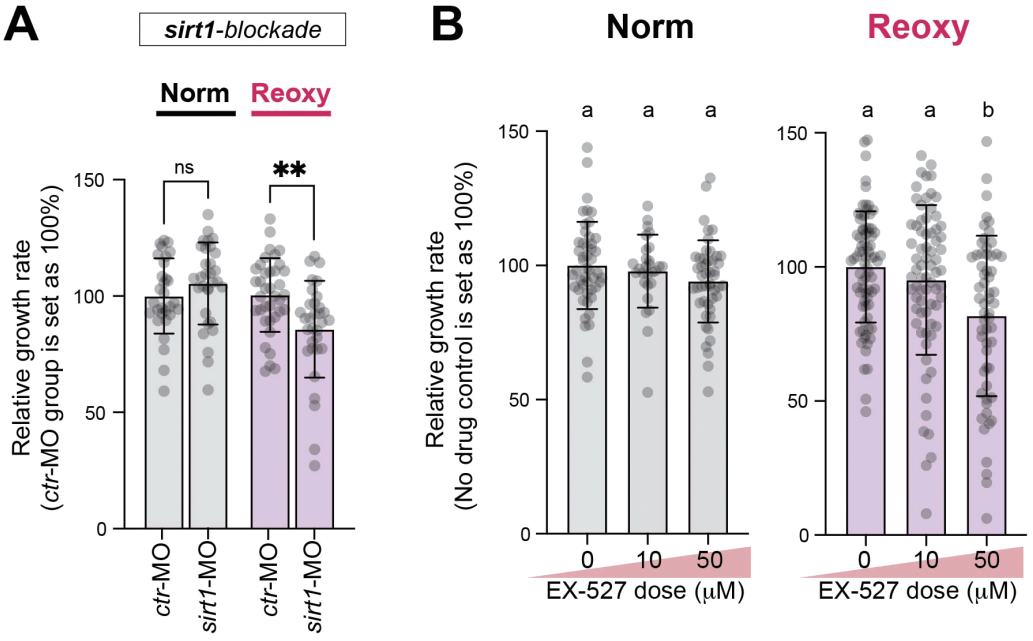

Fig. 2. Effect of specific blockade of *sirt1* on embryonic growth. **(A)** Changes in growth rate of *sirt1*-MO-injected embryos. The relative value is shown. The control group was set as 100. Values are mean ± SD. Data were obtained from three independent assays. n =30 (Norm *ctr*-MO); n = 31 (Norm *sirt1*-MO); n = 37 (Reoxy *ctr*-MO); n = 32 (Reoxy *sirt1*-MO). **: $P < 0.01$; ns: $P > 0.05$. **(B)** Changes in growth rate of the EX-527 (Sirt1-specific inhibitor)-treated embryos in Norm and Reoxy conditions. The control group (DMSO) was set as 100. Values shown are mean ± SD. Data were obtained from two–seven independent assays. n = 48 (Norm DMSO); n = 28 (Norm EX-527 10 μM); n = 48 (Norm EX-527 50 μM); n = 76 (Reoxy DMSO); n = 72 (DMSO EX-527 10 μM); n = 59 (DMSO EX-527 50 μM). Different letters mean statistical significance at $P < 0.05$.

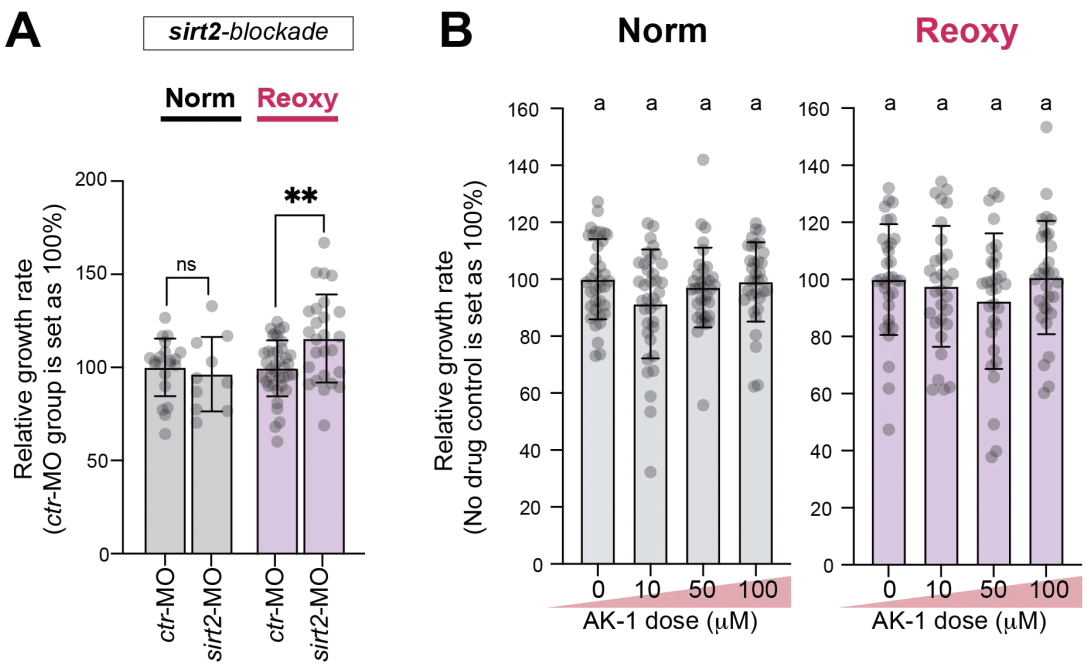

Fig. 3. Effect of specific blockade of *sirt2* on embryonic growth. **(A)** Changes in growth rate of *sirt2*-MO-injected embryos. The relative value is shown. The control group was set as 100. Values are mean ± SD. Data were obtained from two–three independent assays. $n = 21$ (Norm *ctr*-MO); $n = 10$ (Norm *sirt2*-MO); $n = 39$ (Reoxy *ctr*-MO); $n = 26$ (Reoxy *sirt2*-MO). **: $P < 0.01$, ns: $P > 0.05$. **(B)** Changes in growth rate of the AK-1 (Sirt2-specific inhibitor)-treated embryos in Norm and Reoxy conditions. The control group (DMSO) was set as 100. Values shown are mean ± SD. Data were obtained from two independent assays. $n = 36$ (Norm DMSO); $n = 36$ (Norm AK-1 10 μM); $n = 34$ (Norm AK-1 50 μM); $n = 34$ (Norm AK-1 100 μM); $n = 32$ (Reoxy DMSO); $n = 30$ (Reoxy AK-1 10 μM); $n = 30$ (Reoxy AK-1 50 μM); $n = 31$ (Reoxy AK-1 100 μM). The same letter means statistically not significantly different ($P > 0.05$).

S1A). The intact splicing product of *sirt1* cDNA was 249 bps. In contrast, a type of defective *sirt1* cDNA was too long to amplify (2833 bps) in the RT-PCR analysis (see Supplementary Figure S1B). On the other hand, *sirt2*-MO induced defective splicing of the exon 1 and intron 1 boundary (see Supplementary Figure S1C). The PCR product was detected at 413 bps in the *sirt2* MO-injected group, which was different from the original PCR product (236 bps; see Supplementary Figure S1D). Therefore, all of these PCR analyses showed that the MOs used in this study efficiently knocked down *sirt1* and *sirt2*. Next, we tested the growth of the *sirt1* and *sirt2* morphant embryos under the Norm and the Reoxy conditions. We found that the *sirt1* morphants had a significantly reduced growth rate compared to control embryos under the Reoxy condition (83.3 ± 5.9%, Fig. 2). In the Norm condition, however, the growth rate of the *sirt1* morphant was comparable to that of the control embryo. We further tested temporal and dose-dependent inhibition of Sirt1 protein using EX-527. EX-527 remarkably blunted growth in Reoxy embryos (81.3 ± 4.7%, Fig. 2A), though there were no major effects under the Norm condition. On the other hand, the *sirt2* morphant did not change the growth under the Norm condition (Fig. 3A). In the Reoxy condition, the *sirt2* morphant had significantly increased growth rate compared to the control embryo (Fig. 3A). Embryonic growth did not significantly change even at the highest dose (100 μM) of AK-1 in either the Norm or Reoxy conditions (Fig. 3B).

Spatiotemporal expression of *sirt1*

To elucidate the gene expression profile of *sirt1* in catching-up embryos, we prepared cDNA at 36 hpf (Hypo), 42 hpf (Reoxy), and the stage-matched Norm embryos at 26 hpf and 36 hpf (Fig. 4A). The gene expression levels were not significantly different among these embryos (Fig. 4B). We next investigated the spatial expression of *sirt1* by whole-mount in situ hybridization. The *sirt1* expression domains in 26 hpf Norm embryos and 36 hpf Hypo embryos were comparable. The *sirt1* expression was prone to increase globally in 30 hpf Norm embryos and 40 hpf Reoxy embryos, but the distribution patterns were still comparable between the Norm and Reoxy embryos. Notably, in 48 hpf Reoxy embryos, the *sirt1* expression was more prominent in some anterior regions (i.e., pharyngeal arches and midbrain-hindbrain boundary) than in 36 hpf Norm embryos (Fig. 4C). Elsewhere, the *sirt1* expression was detected in the trunk region of both Norm (36 hp) and Reoxy (48 hpf) embryos, where the Reoxy embryos tended to have slightly weaker signals than the Norm embryos (Fig. 4C).

Effect of Sirt1-blockade on the Mapk-activation

To understand the relationship between Sirt1 and the growth signal, we investigated the activation level of Mapk (phosphorylation level of Erk1/2) under the inhibition of Sirt1. Embryos that had experienced 12 hr Hypo treatment were exposed to 50 μM EX-527 for another 12 hours from the beginning of the Reoxy condition (from 36 hpf to 48 hpf). Then, the immunoblot analysis of the embryo lysate revealed the phosphorylation levels of Erk1/2. The stage-matched

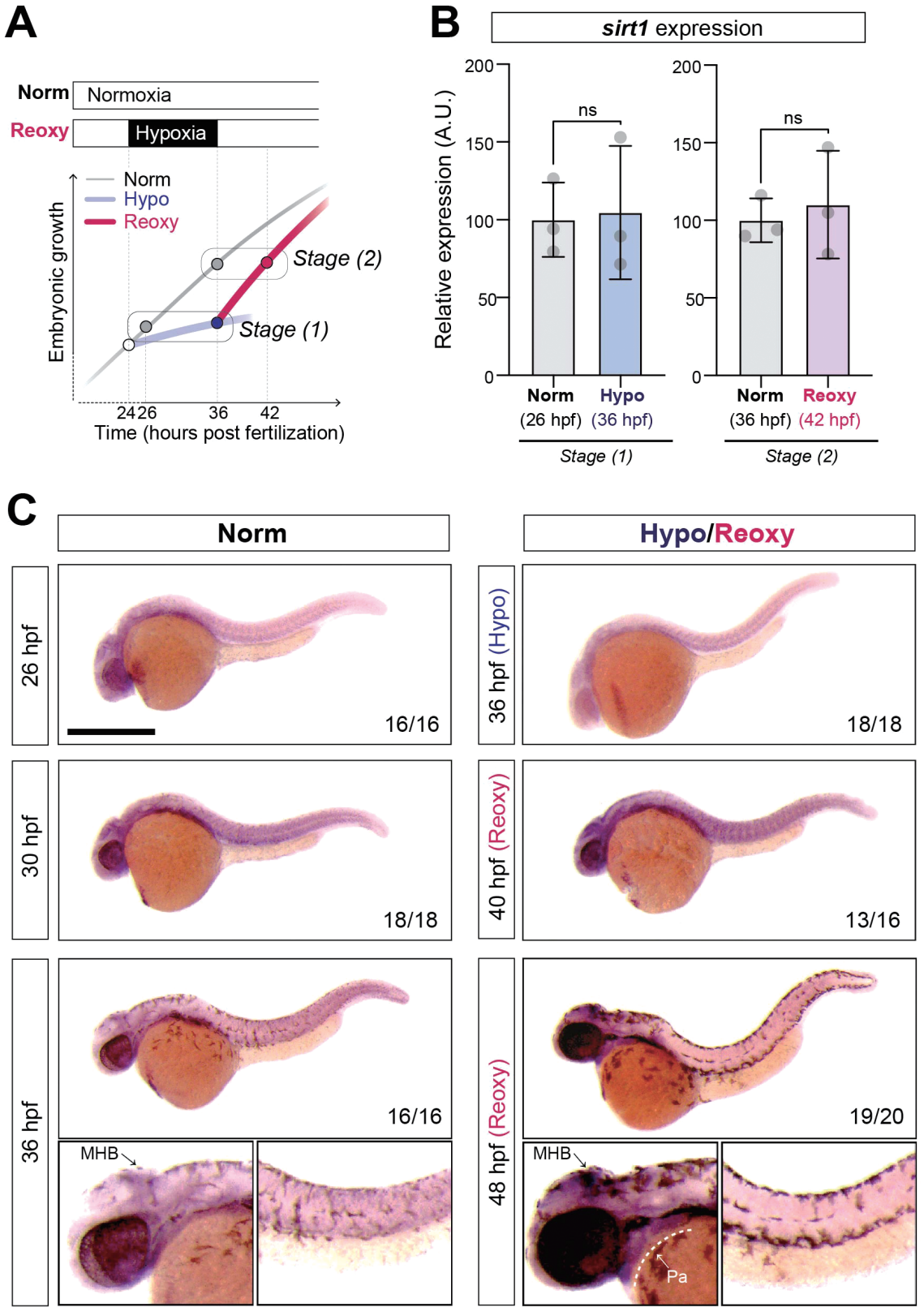

Fig. 4. Spatiotemporal expression of *sirt1*. **(A)** A diagram showing the sampling stages (Stage (1) and (2)) used for gene expression analyses. The total RNAs extracted from Norm, Hypo, and Reoxy embryos were subjected to further gene expression analyses. **(B)** RT-qPCR analysis data. Results are shown as the relative expression levels. The control Norm group value was set as 100. Values shown are mean ± SD. Data were obtained from three independent assays. ns: $P > 0.05$. **(C)** Whole-mount in situ hybridization analysis. Representative results are shown. Bar, 500 μm. Numbers show the penetrance of the representative result. Arrows represent structures with relatively higher staining signals. MHB, midbrain-hindbrain boundary; Pa, pharyngeal arches.

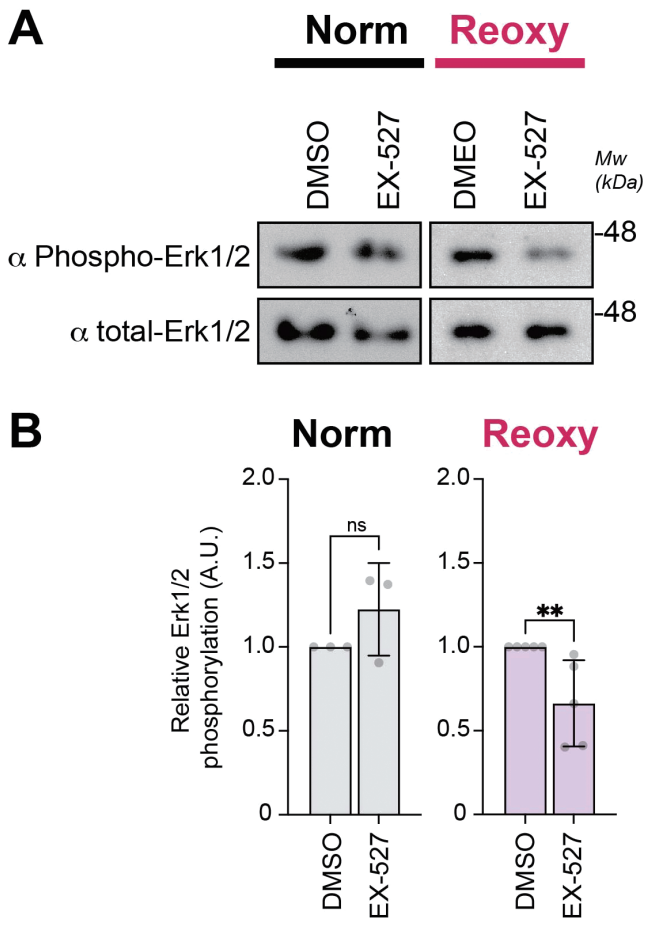

Fig. 5. Effects of Sirt1-blockade on Mapk-activation. **(A)** Representative immunoblotting data. The activation level of Mapk was monitored by measuring relative levels of phospho-Erk1/2. Stage-matched Norm and Reoxy embryos were similarly treated with 50 μM EX-527 and subjected to immunoblot analysis. **(B)** Quantification data of relative Erk1/2 phosphorylation level. The value of control group (DMSO) was set as 1.0. Values shown are mean ± SD. Data were obtained from three–five independent assays. **: $P < 0.01$, ns: $P > 0.05$.

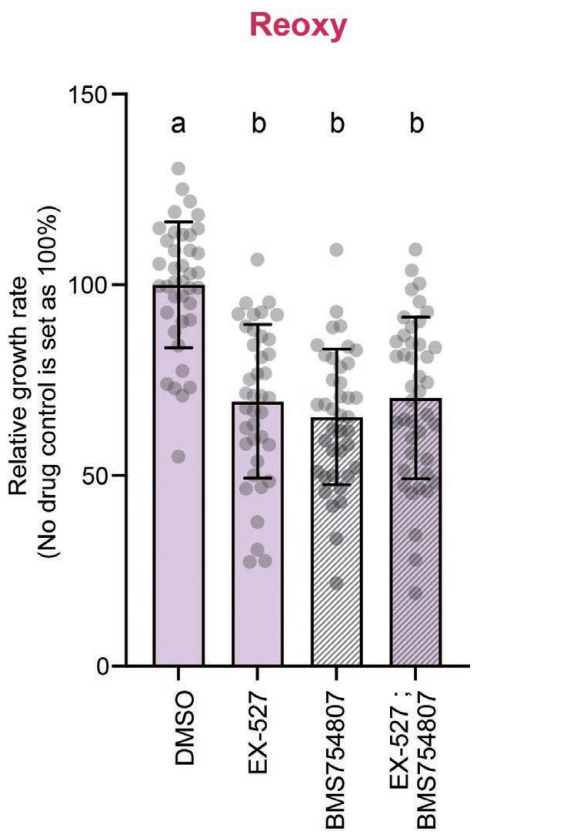

Fig. 6. Effects of Sirt1- and Igf1r-blockade on embryonic growth. Embryos at the beginning of Reoxy (36 hpf) were treated with either 50 μM EX-527, 2 μM BMS754807, or their combination for 12 hr. The head-trunk angle was measured before and after the drug treatments to calculate the relative growth rate. The value of control group (DMSO) was set as 100%. Values shown are mean ± SD. Data were obtained from three independent assays. $n = 39$ (DMSO); $n = 39$ (EX-527); $n = 39$ (BMS754807); $n = 42$ (EX-527; BMS754807). Different letters mean statistical significance at $P < 0.0001$.

Norm embryos were also tested. As results, in the Norm condition, the EX-527 did not reduce the Erk1/2-phosphorylation; however, it significantly decreased the Erk1/2-phosphorylation under the Reoxy condition (Fig. 5A, B). We obtained similar results in the Sirt1/2 blockade experiment using Sirtinol (see Supplementary Figure S2).

Effect of Sirt1- and Igf1r-inhibition on catch-up growth

Since Igf1r signaling plays a major role in the catch-up growth, we examined the relationship between Sirt1 and Igf1r in the Reoxy-induced catch-up growth. The Hypo experienced embryos at 36 hpf were exposed to either 50 μM EX-527, 2 μM BMS754807, or their combination for another 12 hours under the Reoxy condition until 48 hpf. The EX-527 or BMS754807 alone induced significant growth loss compared to the vehicle control (Fig. 6). Importantly, the combination of EX-527 and BMS754807 failed to further reduce the growth of either the EX-527-alone- or the BMS75480-alone-treated embryos (Fig. 6).

Effect of Sirt1- and Igf1r-inhibition on Mapk-activation in catch-up growth

Having identified Sirt1 as an important regulator of Mapk under the Reoxy condition, we investigated the distribution of phospho-Erk1/2 signals in Reoxy embryos by whole-mount immunostaining analysis. In the control embryos, the signal was detected in the head regions, such as the pharyngeal arches, forebrain, midbrain-hindbrain boundary, and a part of the hindbrain (Fig. 7, DMSO, Pa, Fb, MHB, Hb). Also, the signal was observed in the spinal cord and the somite muscle in the trunk (Fig. 7, DMSO, Sc, Sm). Though each inhibitor treatment globally decreased the Erk1/2-phosphorylation level (see references in Supplementary materials online), the reduction was especially prominent in the pharyngeal arches, midbrain-hindbrain boundary, and trunk somiste in both EX-527-alone- and BMS754807-alone-treated embryos compared to the DMSO group. Of note, the combination of EX-527 and BMS754807 did not further reduce the Erk1/2-phosphorylation in either the EX-527-alone- or the BMS754807-alone-treated embryos (Fig. 7: EX-527, BMS754807).

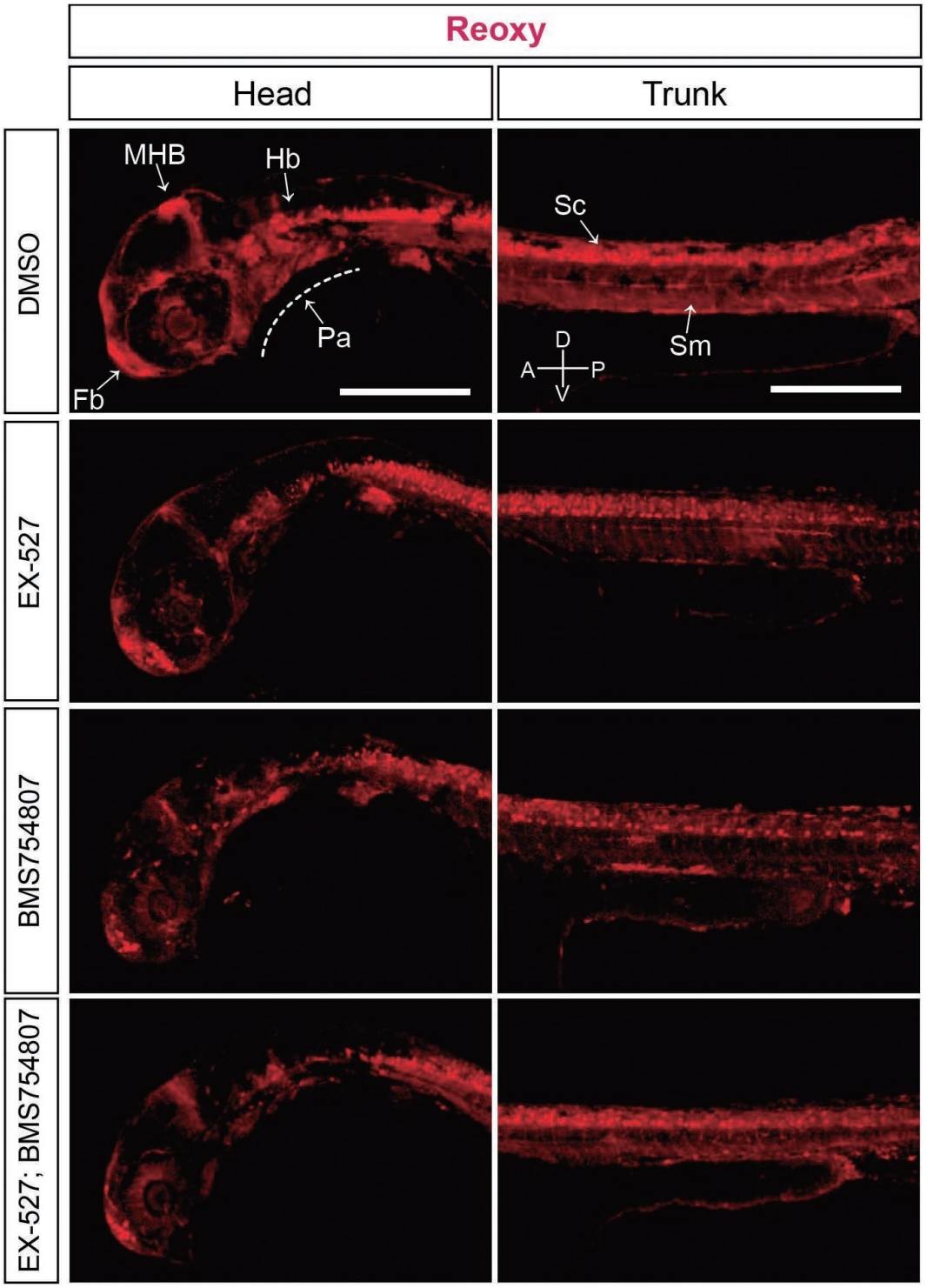

Fig. 7. Effects of Sirt1- and Igf1r-blockade on Mapk activation. Whole-mount immunostaining using anti-phospho-Erk1/2 antibody of drug-treated Reoxy embryos. Embryos at the beginning of Reoxy (36 hpf) were treated with either 50 μM EX-527, 2 μM BMS754807, or their combination for 12 hr, and subjected to the immunostaining experiment. Confocal images of each group of embryos are shown. Arrows indicate stronger phospho-Erk1/2-signals in control specimens. Fb, forebrain; Hb, hindbrain; MHB, midbrain-hindbrain boundary; Pa, pharyngeal arches; Sc, spinal cord; Sm, somite muscle. Directions of the specimen are shown by A(anterior)-P(posterior), D(dorsal)-V(ventral) indicator. Bar, 200 μm.

DISCUSSION

We conceived this study based on the idea that the molecules activated under catabolism are closely related to the induction of catch-up growth. To test this idea, we focused on Sirt1 and its akin paralog, Sirt2, and conducted stage-specific inhibition of these molecules. The results showed that Sirt1 was a prerequisite for catch-up growth (Figs. 1, 2, 6), and it

was a key for the Mapk activation in the Reoxy condition (Fig. 5, 7). Moreover, the Sirt1/Igf1r combinatorial inhibition did not further blunt the Mapk activation or the catch-up growth compared to those in the Igf1r-alone-inhibited groups (Figs. 6, 7), suggesting that the Sirt1 function is linked with Igf1r-induced Mapk activation in the catch-up growth. Sirt1 is particularly linked with the induction of thrifty metabolism, which is known to adapt cells and organisms to catabolic conditions (Sathyanarayan et al., 2017; Lo et al., 2019). We also know that Sirt1 maintains cells in a healthier condition to coordinate cellular metabolism and detox functions leading to slow aging and extending lifespan (Houtkooper et al., 2012; Banerjee et al., 2016; Ren et al., 2017; Kim et al., 2019). In contrast, in a specific setting such as the Reoxy condition, the fact that Sirt1 promotes the growth, which in turn accelerates the physiological age, is intriguing.

Sirtuins are NAD-dependent deacetylases, and their activities are regulated by fluctuating intracellular levels of NAD and ATP, even without changes in their gene expression (Kaeberlein et al., 1999; Imai et al., 2000; Guarente, 2009; Houtkooper et al., 2012). Therefore, in the present study, we started with the pharmacological Sirt1/2 inhibition. As shown by the results, Sirt1/2 inhibition by Sirtinol significantly slowed down the growth in a Reoxy-specific manner (Fig. 1), suggesting that Sirt1 or Sirt2 is, or both are, required for the Reoxy-induced catch-up growth, but not for the growth in the Norm condition. On the other hand, experiments with a Sirt1-selective inhibitor (EX-527) showed that it significantly stunted the growth of Reoxy embryos, while a Sirt2-selective inhibitor (AK-1) had no effect (Figs. 2B, 3B). We also investigated the role of *sirt1/2* using a genetic blockade strategy to corroborate the pharmacological analyses. The results showed that only *sirt1*-suppression in the Reoxy condition significantly reduced the growth compared to the control, while the growth of its Norm counterpart was unchanged (Fig. 2A). There was no change in the growth of *sirt2*-suppressed embryos compared to the control group under Norm conditions (Fig. 3A). On the other hand, inhibition of *sirt2* expression caused a significant increase in growth rate in the Reoxy group. This suggests a possible inhibitory effect of Sirt2 on this growth compensation phenomenon, but the following AK-1 experiment did not show the same results. Thus, it is highly unlikely that Sirt2 promotes catch-up growth, although the role of Sirt2 in catch-up growth needs to be further investigated in the future. Therefore, it was considered that the growth of Reoxy embryos requires Sirt1 action rather than Sirt2 action.

As inhibition of Sirt1/2 in this study did not have a marked effect on normal growth, it is also possible that Sirt1/2 is not significantly involved in embryonic growth under the Norm condition, at least in the stages tested in this study. Previous studies in which *sirt1* expression was inhibited in zebrafish embryos have reported abnormalities in cardiovascular development, but no clear delay in embryonic growth has been described (Potente et al., 2007). However, a recent study revealed that Planaria require SIRT1 for their normal growth and development (Ziman et al., 2020). A study in mice also reported that deletion of the *Sirt1* gene resulted in a clear inhibition of the embryonic growth and postnatal survival (McBurney et al., 2003). Although more careful investigations are needed to decipher the role of Sirt1/2 in normal embryonic growth, our current data suggest that the Sirt1 action is required to promote growth in the catch-up growth more than in normal growth.

We examined the expression levels of *sirt1* by RT-qPCR analysis in Norm, Hypo, and Reoxy conditions (Fig. 4A). Unexpectedly, RT-qPCR analysis revealed no significant changes in *sirt1* expression in any conditions. However, as the cDNAs used for the RT-qPCR analysis came from the whole-body, the spatiotemporal expression of *sirt1* was also investigated by whole-mount in situ hybridization analysis (Fig. 4B). The results showed that the *sirt1* gene was globally expressed with a relatively higher level in some anterior regions of the Reoxy embryos (such as pharyngeal arches and midbrain-hindbrain border region). Importantly, Sirt1-inhibition largely reduced Mapk activation in anterior domains (such as the pharyngeal arches) of Reoxy embryos. The blockade of Igf1r also reduced the activation of Mapk in the same domain. This spatial overlap strongly suggests the functional confluence of the Sirt1 and the Igf1r-Mapk pathways in catch-up growth. Notably, the neural crest cells generate the pharyngeal arches and many other anterior cranial skeletons (Yamauchi et al., 2011; Mongera et al., 2013). Previous studies revealed that neural crest cells play an important role in the catch-up growth in the current experimental model (Kamei et al., 2018). The regulation of *sirt1* expression and its function(s) in neural crest cells and their derivatives could be of great interest to the next research. Analysis of these isolated cells would provide more details on the roles of this gene in catch-up growth.

A recent genetic study in mice showed that *Sirt1* in the epiphysial growth plate or chondrocytes plays a role in the efficient catch-up growth (Shtaif et al., 2020), though how the growth signaling was controlled by the Sirt1 remained elusive. The current study found that inhibition of Sirt1 during catch-up growth reduced the Mapk activation (Fig. 5). In addition, co-inhibition of Sirt1 and Igf1r in Reoxy embryos did not cause further embryonic growth retardation or reduced Erk1/2 phosphorylation compared to the independent inhibition of Igf1r (Figs. 6, 7). These results suggest that one of the important functions of Sirt1 in catch-up growth is to facilitate the Igf1r-Mapk pathway. Previous studies have shown that the Igf1r-Mapk pathway is vital for the rapid growth acceleration in Reoxy embryos (Kamei et al., 2011). In addition, we recently revealed that Irs2b, one of the zebrafish IRS2 orthologs, played a crucial role in the Igf1r-Erk1/2 activation only under the Reoxy condition (Zasu et al., 2022). Another report of a study in a mammalian model showed that Sirt1 activated the IGF1R-Erk1/2 pathway via the deacetylation of IRS2 (Li et al., 2008). The precise molecular mechanism by which Irs2b and Sirt1 cooperate to promote the Igf1r-Mapk pathway in the zebrafish model awaits future study.

The Sirt1-induced Mapk activation likely occurs at the plasma membrane or cytosol; however, the Sirt1 function in the nucleus should not be ignored. Importantly, the primary subcellular localization of Sirt1 is known to be the nucleus, where it regulates chromatin states and expression of various genes (Guarente, 2009; Houtkooper et al., 2012). Sirt1 deacetylates a number of nucleus-resident proteins that change cellular metabolism and fates. The Mapk-effectors in the nucleus (including transcription factors) could collabo-

rate with nuclear Sirt1 target proteins. Another plausible scenario is that the nuclear function of Sirt1 alters the role of the Mapk-effectors. Indeed, a number of nuclear resident molecules (such as c-Myc and Histone H1) are under regulation by both Sirt1 and Mapk (Chadee et al., 1995; Vaquero et al., 2004; Gordan et al., 2007a, b). Further analysis of the Sirt1 function(s) in the nucleus during catch-up growth would lead to better understanding of the functional nexus of the Sirt1 and mitogenic signaling ignited by endocrine factors.

ACKNOWLEDGMENTS

We thank Mr. Futa Hishima and Ms. Mayu Mizuno for their technical instructions. This work was supported by the Japan Society for the Promotion of Science, Grant-in-Aid for Scientific Research (C) (18K06014); Grant-in-Aid for Scientific Research (B) (23H02172) to HK, and Grant-in-Aid for JSPS Fellows (22J00232) to OH.

COMPETING INTERESTS

The authors declare no competing interests.

AUTHOR CONTRIBUTIONS

HK designed the research; OH, MS, and HK performed experiments; OH, MS, and HK wrote the draft. OH and HK reviewed and edited the manuscript.

SUPPLEMENTARY MATERIALS

Supplementary materials for this article are available online. (URL: https://doi.org/10.2108/zs230059)

Supplementary Figure S1. Gene specific blockade of *sirt1* and *sirt2*. **(A)** Schematic illustration of *sirt1*-MO function on its target RNA. MOs affect proper splicing at the exon 2-intron 2 boundary. As a result, truncated splicing variant mRNA was generated. **(B)** Representative result of RT-PCR analysis of *sirt1* expression. **(C)** Schematic illustration of *sirt2*-MO function on its target RNA. MOs affect proper splicing at the exon 1-intron 1 boundary. As a result, truncated splicing variant mRNA was generated. **(D)** Representative result of RT-PCR analysis of *sirt2* expression.

Supplementary Figure S2. Effect of Sirt1/2-blockade on Mapk-activation **(A)** Representative immunoblotting data. The activation level of Mapk was monitored by measuring relative levels of phospho-Erk1/2. Stage-matched embryos in Norm and Reoxy conditions were similarly treated with 50 μM Sirtinol for 12 hr and then subjected to immunoblot analysis. **(B)** Quantification data of relative Erk1/2 phosphorylation level. The value of the control group (DMSO) was set as 1.0. Values shown are mean ± SD. Data were obtained from three–five independent assays. *: $P < 0.05$, ns: $P > 0.05$.

Supplementary Figure S3. Effects of Sirt1- and Igf1r-blockade on Mapk activation Whole-mount immunostaining of drug-treated Reoxy embryos using anti-phospho-Erk1/2 antibody. Embryos at the beginning of Reoxy (36 hpf) were treated with either 50 μM EX-527, 2 μM BMS754807, or their combination, for 12 hr, and subjected to the immunostaining experiment. Confocal images of each group of embryos are shown. Directions of the specimens are shown by A(anterior)-P(posterior) and D(dorsal)-V(ventral) indicators. Bar, 200 μm. (These images are the whole-body images of the data in Fig. 7.)

REFERENCES

Banerjee J, Bruckbauer A, Zemel MB (2016) Activation of the AMPK/Sirt1 pathway by a leucine-metformin combination increases insulin sensitivity in skeletal muscle, and stimulates glucose and lipid metabolism and increases life span in *Caenorhabditis elegans*. Metabolism 65: 1679–1691

Berendsen AD, Olsen BR (2015) Bone development. Bone 80: 14–18

Cabello G, Wrutniak C (1989) Thyroid hormone and growth: relationships with growth hormone effects and regulation. Reprod Nutr Dev 29: 387–402

Chadee DN, Taylor WR, Hurta RA, Allis CD, Wright JA, Davie JR (1995) Increased phosphorylation of histone H1 in mouse fibroblasts transformed with oncogenes or constitutively active mitogen-activated protein kinase kinase. J Biol Chem 270: 20098–20105

Chang HC, Guarente L (2014) SIRT1 and other sirtuins in metabolism. Trends Endocrinol Metab 25: 138–145

Clemmons DR (2018) Role of IGF-binding proteins in regulating IGF responses to changes in metabolism. J Mol Endocrinol 61: 139–169

Gat-Yablonski G, Phillip M (2015) Nutritionally-induced catch-up growth. Nutrients 7: 517–551

Gordan JD, Bertout JA, Hu CJ, Diehl JA, Simon MC (2007a) HIF-2alpha promotes hypoxic cell proliferation by enhancing c-myc transcriptional activity. Cancer Cell 11: 335–347

Gordan JD, Thompson CB, Simon MC (2007b) HIF and c-Myc: sibling rivals for control of cancer cell metabolism and proliferation. Cancer Cell 12: 108–113

Guarente L (2009) Hypoxic hookup. Science 324: 1281–1282

Houtkooper RH, Pirinen E, Auwerx J (2012) Sirtuins as regulators of metabolism and healthspan. Nat Rev Mol Cell Biol 13: 225–238

Imai S, Armstrong CM, Kaeberlein M, Guarente L (2000) Transcriptional silencing and longevity protein Sir2 is an NAD-dependent histone deacetylase. Nature 403: 795–800

Kaeberlein M, McVey M, Guarente L (1999) The SIR2/3/4 complex and SIR2 alone promote longevity in *Saccharomyces cerevisiae* by two different mechanisms. Genes Dev 13: 2570–2580

Kajimura S, Aida K, Duan C (2005) Insulin-like growth factor-binding protein-1 (IGFBP-1) mediates hypoxia-induced embryonic growth and developmental retardation. Proc Natl Acad Sci U S A 102: 1240–1245

Kamei H (2020) Oxygen and embryonic growth: the role of insulin-like growth factor signaling. Gen Comp Endocrinol 294: 113473

Kamei H, Duan C (2018) Hypoxic treatment of zebrafish embryos and larvae. Methods Mol Biol 1742: 195–203

Kamei H, Lu L, Jiao S, Li Y, Gyrup C, Laursen LS, et al. (2008) Duplication and diversification of the hypoxia-inducible IGFBP-1 gene in zebrafish. PLOS ONE 3: e3091

Kamei H, Ding Y, Kajimura S, Wells M, Chiang P, Duan C (2011) Role of IGF signaling in catch-up growth and accelerated temporal development in zebrafish embryos in response to oxygen availability. Development 138: 777–786

Kamei H, Yoneyama Y, Hakuno F, Sawada R, Shimizu T, Duan C, et al. (2018) Catch-up growth in zebrafish embryo requires neural crest cells sustained by Irs1signaling. Endocrinology 159: 1547–1560

Kim DH, Jung IH, Kim DH, Park SW (2019) Knockout of longevity gene Sirt1 in zebrafish leads to oxidative injury, chronic inflammation, and reduced life span. PLOS ONE 14: e0220581

Kimmel CB, Ballard WW, Kimmel SR, Ullmann B, Schilling TF (1995) Stages of embryonic development of the zebrafish. Dev Dyn 203: 253–310

Kincaid B, Bossy-Wetzel E (2013) Forever young: SIRT3 a shield against mitochondrial meltdown, aging, and neurodegeneration. Front Aging Neurosci 5: 48

Kraemer WJ, Ratamess NA, Hymer WC, Nindl BC, Fragala MS (2020) Growth hormone(s), testosterone, insulin-like growth factors, and cortisol: Roles and integration for cellular development and growth with exercise. Front Endocrinol (Lausanne) 11: 33

Lee D, Goldberg AL (2013) SIRT1 protein, by blocking the activities

of transcription factors FoxO1 and FoxO3, inhibits muscle atrophy and promotes muscle growth. J Biol Chem 288: 30515–30526

Li Y, Xu W, McBurney MW, Longo VD (2008) SirT1 inhibition reduces IGF-I/IRS-2/Ras/ERK1/2 signaling and protects neurons. Cell Metab 8: 38–48

Lo MC, Chen JY, Kuo YT, Chen WL, Lee HM, Wang SG (2019) Camptothecin activates SIRT1 to promote lipid catabolism through AMPK/FoxO1/ATGL pathway in C(2)C(12) myogenic cells. Arch Pharm Res 42: 672–683

Madsen AS, Andersen C, Daoud M, Anderson KA, Laursen JS, Chakladar S, et al. (2016) Investigating the sensitivity of NAD+-dependent sirtuin deacylation activities to NADH. J Biol Chem 291: 7128–7141

McBurney MW, Yang X, Jardine K, Hixon M, Boekelheide K, Webb JR, et al. (2003) The mammalian SIR2alpha protein has a role in embryogenesis and gametogenesis. Mol Cell Biol 23: 38–54

Michishita E, Park JY, Burneskis JM, Barrett JC, Horikawa I (2005) Evolutionarily conserved and nonconserved cellular localizations and functions of human SIRT proteins. Mol Biol Cell 16: 4623–4635

Mongera A, Singh AP, Levesque MP, Chen YY, Konstantinidis P, Nusslein-Volhard C (2013) Genetic lineage labeling in zebrafish uncovers novel neural crest contributions to the head, including gill pillar cells. Development 140: 916–925

Osborne TB, Mendel LB (1915) The resumption of growth after long continued failure to grow. J Biol Chem 23: 439–454

Potente M, Ghaeni L, Baldessari D, Mostoslavsky R, Rossig L, Dequiedt F, et al. (2007) SIRT1 controls endothelial angiogenic functions during vascular growth. Genes Dev 21: 2644–2658

Ren J, Yang L, Zhu L, Xu X, Ceylan AF, Guo W, et al. (2017) Akt2 ablation prolongs life span and improves myocardial contractile function with adaptive cardiac remodeling: role of Sirt1-mediated autophagy regulation. Aging Cell 16: 976–987

Rifai K, Judes G, Idrissou M, Daures M, Bignon YJ, Penault-Llorca F, et al. (2018) SIRT1-dependent epigenetic regulation of H3 and H4 histone acetylation in human breast cancer. Oncotarget 9: 30661–30678

Saenger P, Czernichow P, Hughes I, Reiter EO (2007) Small for gestational age: short stature and beyond. Endocr Rev 28: 219–251

Sathyanarayan A, Mashek MT, Mashek DG (2017) ATGL promotes autophagy/lipophagy via SIRT1 to control hepaticLipid droplet catabolism. Cell Rep 19: 1–9

Sauve AA (2010) Sirtuins. Biochim Biophys Acta 1804: 1565–1566

Shtaif B, Bar-Maisels M, Gabet Y, Hiram-Bab S, Yackobovitch-Gavan M, Phillip M, et al. (2020) Cartilage-specific knockout of Sirt1 significantly reduces bone quality and catch-up growth efficiency. Bone 138: 115468

Vaquero A, Scher M, Lee D, Erdjument-Bromage H, Tempst P, Reinberg D (2004) Human SirT1 interacts with histone H1 and promotes formation of facultative heterochromatin. Mol Cell 16: 93-105

Wit JM, Boersma B (2002) Catch-up growth: definition, mechanisms, and models. J Pediatr Endocrinol Metab 15 Suppl 5: 1229–1241

Yamauchi H, Goto M, Katayama M, Miyake A, Itoh N (2011) Fgf20b is required for the ectomesenchymal fate establishment of cranial neural crest cells in zebrafish. Biochem Biophys Res Commun 409: 705–710

Zasu A, Hishima F, Thauvin M, Yoneyama Y, Kitani Y, Hakuno F, et al. (2022) NADPH-oxidase derived hydrogen peroxide and Irs2b facilitate re-oxygenation-induced catch-up growth in zebrafish embryo. Front Endocrinol (Lausanne) 13: 929668

Ziman B, Karabinis P, Barghouth P, Oviedo NJ (2020) Sirtuin-1 regulates organismal growth by altering feeding behavior and intestinal morphology in planarians. J Cell Sci 133: jcs239467

(Received June 29, 2023 / Accepted September 23, 2023 / Published online November 29, 2023)